MECSOL 2019 - Proceedings of the 7th International Symposium on Solid Mechanics
V. Tita, A. Ferreira, M.L. Ribeiro, A. Vieira and A.T. Beck (Editors), ABCM, Sao Carlos, SP, Brazil, April 15th to 17th, 2019

Hierarchical methods for free vibration of thin curved beams

Ramon Macedo Corrêa[1], Marcos Arndt[1] and Roberto Dalledone Machado[1]

[1] Federal University of Paraná, Postgraduate Program in Civil Construction Engineering, Mailbox 19011 - CEP 81531-990, Curitiba, PR, Brazil.

Abstract. In this paper the use of hierarchical methods for free vibration of thin curved beams is explored. Two hierarchical approaches using the Generalized Finite Element Method and the Hierarchical Finite Element Method are proposed. Free vibration analyses using these two approaches and the hierarchical Fourier p-element available in literature are performed in order to obtain the natural frequencies of circular rings, modeling one quarter of ring by taking advantage of ring symmetry. Convergence tests of the natural frequencies are performed and the responses of the three methods are compared with analytical solution found in the literature. It is also evaluated the evolution of the mass matrix's condition number with the increase of the refinement. A second model of a pinned-pinned arch is evaluated to prove the methods efficiency.
Keywords: Free Vibration, Thin curved beams, Hierarchical methods.

INTRODUCTION

The free vibration analysis looks for the dynamic characteristics of the structure, such as the natural frequencies. Numerical methods can be used to solve the mathematical problem related to this analysis.

According to Campion and Jarvis (1996) major benefits of the hierarchical *p*-method are the retention of the stiffness coefficients as the order of interpolation is increased and the high rates of convergence possible without the need for mesh refinement. These benefits promote a decreasing in the computational effort involved.

The first hierarchical method explored in this paper is the Generalized Finite Element Method (GFEM), which was independently proposed by several authors (Melenk and Babuska, 1996; Duarte and Oden, 1996; Oden, Duarte and Zienkiewicz, 1998; Duarte, Babuska and Oden, 2000; Babuska, Banerjee and Osborn, 2004). This method is based on the Partition of Unit Method, which is used to expand the traditional Finite Element Method approximation space. The GFEM has been successfully applied to dynamic problems of framed structures as shown in Arndt, Machado and Scremin (2010), Torii and Machado (2012), Weinhardt, Arndt and Machado (2016), among other works.

The second hierarchical method studied here is the Hierarchical Finite Element Method (HFEM) using the Bardell and Lobatto's polynomials for the hierarchical *p* refinement.

The third hierarchical method is the Fourier p-element which was proposed in Leung and Chan (1998) and used for free vibration analyses of thin and thick curved beams in Leung and Zhu (2004). In this paper these methods are applied for free vibration analyses of thin curved beams.

According to Leung and Zhu (2004), the interest of researchers in curved beam elements has been increased for two main reasons: the first is the increased use of such structural element and the second is that the understanding of its behavior provides a view of various aspects of shell elements behavior.

Petyt and Fleischer (1971) presents three finite element models for determining the radial vibrations of curved beam. Their investigations showed that the most accurate results are obtained when both the normal and tangential displacements are approximated by cubic polynomials. Dawe (1974) and Raveendranath, Singh and Pradhan (2000) presented several finite element models using different and higher polynomial orders to approximate the normal and tangential displacements.

In this paper these methods are applied for free vibration analyses of thin curved beams and their efficiency is analyzed and compared to each other.

HIERARCHICAL FINITE ELEMENT METHODS

In the hierarchical methods the approximate displacements response can be written as:

$$u_{apr} = \sum_{i=1}^{n} N_i \, a_i \tag{1}$$

where N_i are the shape functions and a_i are the related degrees of freedom. Note that degrees of freedom are not necessarily

related to nodes. The approximation is hierarchical if an increase from n to $n+1$ does not change the N_i shape functions ($i = 1$ to n).

Dividing the displacement response into two plots, the first related to nodal degrees of freedom (u_{FEM}) and the second related to the non nodal degrees of freedom (here called field degrees of freedom) (u_{ENR}), Eq. (1) becomes:

$$u_{apr} = u_{FEM} + u_{ENR} \tag{2}$$

with:

$$u_{FEM} = \sum_{i=1}^{n} F_i u_i \tag{3}$$

where F_i are classical FEM shape functions and u_i the nodal nodal degrees of freedom related to F_i, and the u_{ENR} depends of the hierarchical method employed.

SHAPE FUNCTIONS

In this section the C^0 and C^1 shape functions are presented. The shape functions related to the field degrees of freedom depend on the method employed.

C^0 shape functions

The traditional FEM shape functions used in this element are the Lagrange linear polynomials, which are described by the following expressions in the interval $[-1,1]$:

$$F_1 = \frac{1-\xi}{2} \tag{4}$$

$$F_2 = \frac{1+\xi}{2} \tag{5}$$

C^0 p-Fourier Element shape functions

The p-Fourier element C^0 was proposed by Leung and Chan (1998) and used for curved beam element in Leung and Zhu (2004). Its enrichment functions are describe by in the domain of $[-1,1]$ by:

$$\Phi_i = \sin\left[i\pi\left(\frac{\xi+1}{2}\right)\right],\ i = 1,2,...,nl \tag{6}$$

where nl is the number of enrichment levels. The u_{ENR} parcel in this method is:

$$u_{ENR} = \sum_{i=0}^{nl} \Phi_i b_i \tag{7}$$

where b_i are the field degrees of freedom related to Φ_i.

C^0 GFEM shape functions

The proposed C^0 GFEM uses the enrichment functions which were used by Leung and Zhu (2004) for thin curved beam described in Eq. (6).

In Leung and Zhu (2004) the enrichment functions are used directly as shape functions, whereas in this paper the GFEM shape functions are first multiplied for a Partition of Unit, then the GFEM u_{ENR} parcel becomes:

$$u_{ENR} = \sum_{i=1}^{2} \eta_i \left(\sum_{j=1}^{nl} \Phi_j b_{ij}\right) \tag{8}$$

where η_i are the partition of unit functions, which in this paper are the Lagrange linear polynomial, described as:

$$\eta_1 = \frac{1-\xi}{2} \tag{9}$$

$$\eta_2 = \frac{1+\xi}{2} \tag{10}$$

C^0 HFEM shape functions

For the C^0 HFEM, the functions used for the p refinement are the Lobatto polynomials, which are obtained by the following expression, in the interval $[-1,1]$:

$$l_k(x) = \frac{1}{||L_{k-1}||_2} \int_{-1}^{x} L_{k-1}(\xi)\, d\xi \tag{11}$$

$$||L_{k-1}||_2 = \int_{-1}^{1} L_{k-1}^2(x)\, dx = \sqrt{\frac{2}{2k-1}} \quad \text{and} \quad k \geq 3 \tag{12}$$

where L_k are:

$$\begin{aligned} &L_0(x) = 1; \\ &L_1(x) = x; \\ &L_k(x) = \frac{2k-1}{k}\, x L_{k-1}(x) - \frac{k-1}{k} L_{k-2} \qquad k \geq 2 \end{aligned} \tag{13}$$

The u_{ENR} parcel in HFEM is:

$$u_{ENR} = \sum_{i=0}^{nl} l_{i+2}\, b_i \tag{14}$$

C^1 shape functions

The traditional FEM shape functions used in this element are the Hermite cubic polynomials, described by the following expressions in the interval $[-1,1]$:

$$F_1 = \frac{1}{2} - \frac{3}{4}\xi + \frac{1}{4}\xi^3 \tag{15}$$

$$F_2 = \frac{L_e}{8}(1 - \xi - \xi^2 + \xi^3) \tag{16}$$

$$F_3 = \frac{1}{2} + \frac{3}{4}\xi - \frac{1}{4}\xi^3 \tag{17}$$

$$F_4 = \frac{L_e}{8}(-1 - \xi + \xi^2 + \xi^3) \tag{18}$$

where L_e is the element length.

C^1 p-Fourier Element shape functions

The p-Fourier element C^1 was proposed by Leung and Chan (1998) and used for curved beam element in Leung and Zhu (2004). p-Fourier enrichment shape functions are describe by in the domain of $[-1,1]$ by:

$$\Phi_i = \left(\frac{1-\xi^2}{4}\right) \sin\left[i\pi\left(\frac{\xi+1}{2}\right)\right], \; i = 1,2,...,nl \tag{19}$$

In this case the u_{ENR} parcel is the same described in Eq. (7).

C^1 GFEM shape functions

The proposed C^1 GFEM uses the enrichment functions which were used by Leung and Zhu (2004) for thin curved beam described in Eq. (19).

In Leung and Zhu (2004) the enrichment functions are used directly as shape functions, whereas in this paper the C^1 GFEM shape functions are multiplied by Partition of Unit functions, the GFEM u_{ENR} parcel is again described by Eq. (8).

C[1] HFEM shape functions

For the C[1] HFEM, the shape functions used for the p refinement are the cubic Hermite polynomials (Eqs. (15) to (18)) associated with the Bardell polynomials, obtained by the following expression, in the interval $[-1,1]$:

$$f_r(\xi) = \sum_{n=0}^{r/2} \frac{(-1)^n (2r-2n-7)!!}{2^n n!(r-2n-1)!} \xi^{r-2n-1} \tag{20}$$

where $r!! = r(r-2)\cdots(2 \text{ or } 1)$, $0!! = (-1)!! = 1$, $r/2$ denotes its own integer part, and $k \geq 5$.

The HFEM u_{ENR} parcel is:

$$u_{ENR} = \sum_{i=0}^{nl} f_{i+4}\, b_i \tag{21}$$

THIN CURVED BEAM ELEMENT

The thin curved beam element was developed by Dawe (1974), Raveendranath, Singh and Pradhan (2000), and Leung and Zhu (2004). They describe extensional strain (ε), rotation (ϕ) and change of curvature (χ) in terms of the displacements and their derivatives according to classical thin shell theory, as shown in the following expressions:

$$\varepsilon = \frac{du}{ds} + \frac{w}{R}, \tag{22}$$

$$\phi = \frac{u}{R} - \frac{dw}{ds}, \tag{23}$$

$$\chi = \frac{1}{R}\frac{du}{ds} - \frac{d^2w}{ds^2}, \tag{24}$$

where R is the radius of the curved beam, u and w are the tangential and normal components of the displacement at s, respectively, and s is the curvilinear coordinate, as represented in Fig. 1.

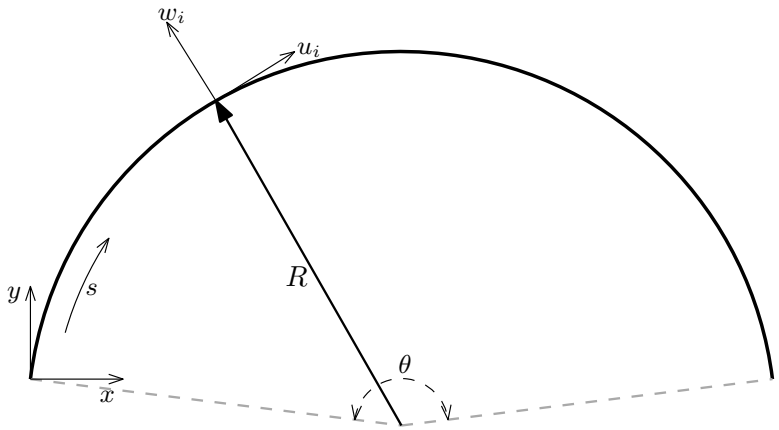

Figure 1 – Curved beam geometry.

The rotation (ϕ) and change of curvature (χ) are represented in Fig. 2 and 3.

The strain energy (U) and kinetic energy (T) expressions are written as:

$$U = \frac{1}{2}\int_0^{L_e} (EA\varepsilon^2 + EI\chi^2)\, ds, \tag{25}$$

$$T = \frac{1}{2}\int_0^{L_e} \rho A\,(\dot{u}^2 + \dot{w}^2)\, ds, \tag{26}$$

where E is the Young's modulus, A is the cross-sectional area, I is the moment of inertia and ρ is the material density. The displacements fields can be written as:

$$u = \sum P_i u_i \text{ and } w = \sum Q_i w_i, \tag{27}$$

where P_i and Q_i are the shape functions related to u and w, respectively, and u_i and w_i are the degrees of freedom also related to u and w, respectively. The P_i and Q_i shape functions are, respectively, the C^0 and C^1 shape functions.

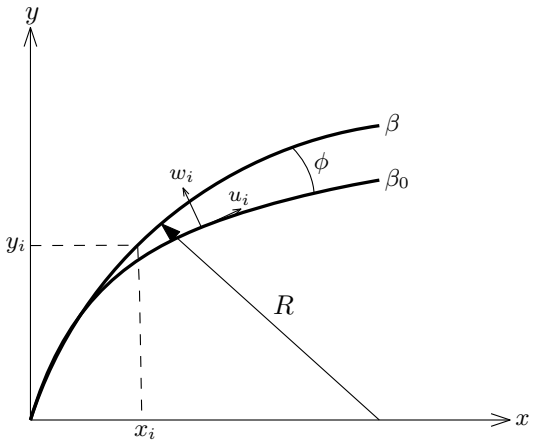

Figure 2 – Rotation (ϕ) of curved beam element.

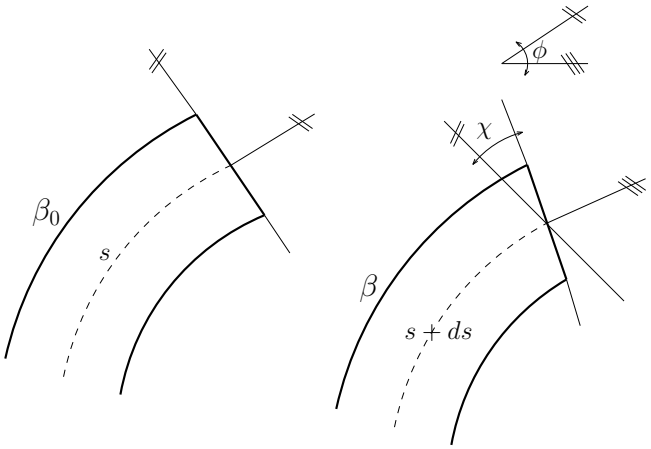

Figure 3 – Rotation (ϕ) and change of curvature (χ) of curved beam element.

Being $\{\mathbf{q}\}$ a vector containing the degrees of freedom related to u and w as shown below:

$$\{\mathbf{q}\} = \begin{Bmatrix} u_1 \\ \vdots \\ u_n \\ w_1 \\ \vdots \\ w_n \end{Bmatrix} \tag{28}$$

and $\{\mathbf{N_P}\}$ a vector formed by the shape functions P_i and $\{\mathbf{N_Q}\}$ a vector formed by the shape functions Q_i:

$$\{\mathbf{N_P}\} = \begin{Bmatrix} P_1 \\ P_2 \\ \vdots \\ P_n \end{Bmatrix} \text{ and } \{\mathbf{N_Q}\} = \begin{Bmatrix} Q_1 \\ Q_2 \\ \vdots \\ Q_n \end{Bmatrix} \tag{29}$$

and still writing:

$$\left\{\overline{\mathbf{N_P}}\right\} = \begin{Bmatrix} \mathbf{N_P} \\ 0 \\ \vdots \\ 0 \end{Bmatrix} \text{ and } \left\{\overline{\mathbf{N_Q}}\right\} = \begin{Bmatrix} 0 \\ \vdots \\ 0 \\ \mathbf{N_Q} \end{Bmatrix} \tag{30}$$

in such a way that $\left\{\overline{\mathbf{N_P}}\right\}$ and $\left\{\overline{\mathbf{N_Q}}\right\}$ have the same size and that it is equal to the size of $\{\mathbf{q}\}$. The displacement fields can then be described as:

$$u = \left\{\overline{\mathbf{N_P}}\right\}^T \{\mathbf{q}\} \text{ and } w = \left\{\overline{\mathbf{N_Q}}\right\}^T \{\mathbf{q}\} \tag{31}$$

The Euler-Lagrange expression becomes:

$$L = T - U = \frac{1}{2}\left(\{\dot{\mathbf{q}}\}^T [\mathbf{M}] \{\dot{\mathbf{q}}\} - \{\mathbf{q}\}^T [\mathbf{K}] \{\mathbf{q}\}\right) \tag{32}$$

Minimizing the energy functional, the equation of motion for undamped free vibration is obtained in the matrix form:

$$[\mathbf{M}]\{\ddot{\mathbf{q}}\} + [\mathbf{K}]\{\mathbf{q}\} = 0 \tag{33}$$

where $\{\mathbf{q}\} = \left\{ \begin{array}{cc} u_i & w_i \end{array} \right\}^T$, $[\mathbf{M}]$ is the mass matrix and $[\mathbf{K}]$ is the stiffness matrix.

The Eq. (33) results in the generalized eigenvalues and eigenvectors problem, described by the expression:

$$([\mathbf{K}] - \lambda^2[\mathbf{M}])\{\boldsymbol{\varphi}\} = 0 \tag{34}$$

where λ are the natural frequencies of vibration and $\{\boldsymbol{\varphi}\}$ are the modes of vibration. The elementary stiffness and mass matrices in Eq. (34) are described by the following expressions:

$$\mathbf{K}^e_{ij} = \int_0^{L_e} \left\{ \begin{array}{c} \dfrac{dP_i}{ds} + \dfrac{Q_i}{R} \\ \\ \dfrac{1}{R}\dfrac{dP_i}{ds} - \dfrac{d^2Q_i}{ds^2} \end{array} \right\}^T \left[\begin{array}{cc} EA & 0 \\ 0 & EI \end{array} \right] \left\{ \begin{array}{c} \dfrac{dP_j}{ds} + \dfrac{Q_j}{R} \\ \\ \dfrac{1}{R}\dfrac{dP_j}{ds} - \dfrac{d^2Q_j}{ds^2} \end{array} \right\} ds \tag{35}$$

$$\mathbf{M}^e_{ij} = \int_0^{L_e} \rho A \left\{ \begin{array}{c} P_i \\ Q_i \end{array} \right\}^T \left\{ \begin{array}{c} P_j \\ Q_j \end{array} \right\} ds \tag{36}$$

NUMERICAL RESULTS

In order to evaluate the results obtained by the hierarchical methods, the free vibration of a circular ring and a pinned-pinned arch are analyzed, to increase the number of degrees of freedom only the *p* refinement is done in both examples. The p-Fourier element was developed in Leung and Zhu (2004) and it was call as THIN^{01}.

Ring's model

As Timoshenko (1955) presents an analytical solution for a ring's natural frequencies and taking advantage of the ring's symmetry, only one quarter of it is modeled with symmetrical boundary conditions. Thus only the even frequencies of the ring are obtained. The ring's scheme is shown in Fig. 4.

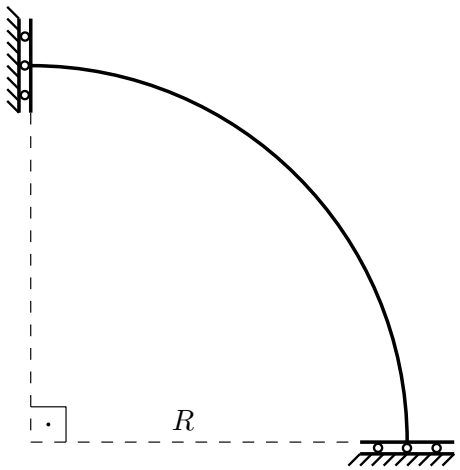

Figure 4 – Quarter ring scheme.

The modeled ring has the following properties: cross-section 0.9525mm x 0.9525mm, radius of curvature of 0.3048m, material density of 1827.44 kg/m^3 and Young's modulus of 1.31×10^{11} N/m^2. The convergence of the first four even frequencies obtained by the three methods are shown in Fig. 5, 6, 7 and 8.

The GFEM is the one with the best convergence rate for this model, second in relation to the convergence rate is the HFEM, both the methods converge to the same values in the first four evaluated frequencies.

In Fig. 9 the evolution of the mass matrix's condition number is shown as the number of enrichment level is increased.

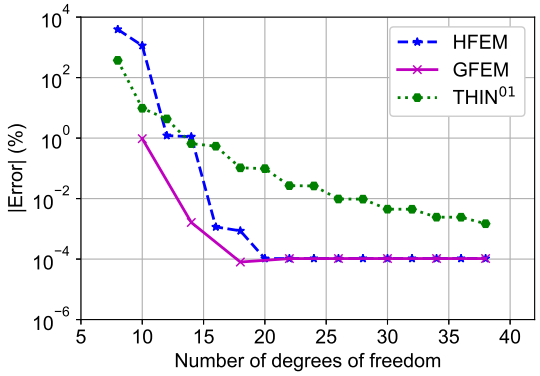

Figure 5 – Convergence of the second frequency of the ring.

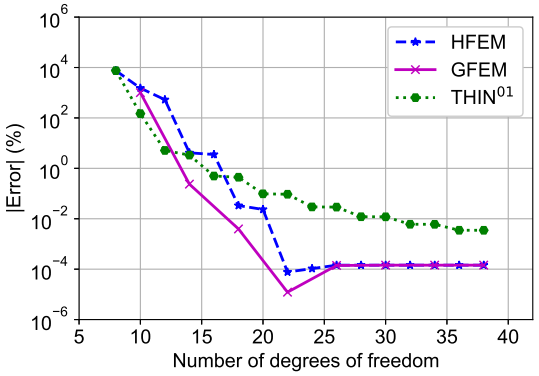

Figure 6 – Convergence of the fourth frequency of the ring.

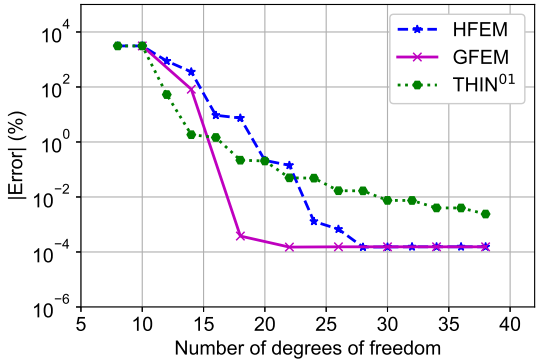

Figure 7 – Convergence of the sixth frequency of the ring.

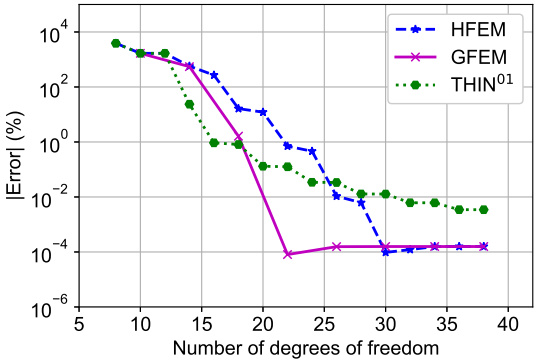

Figure 8 – Convergence of the eighth frequency of the ring.

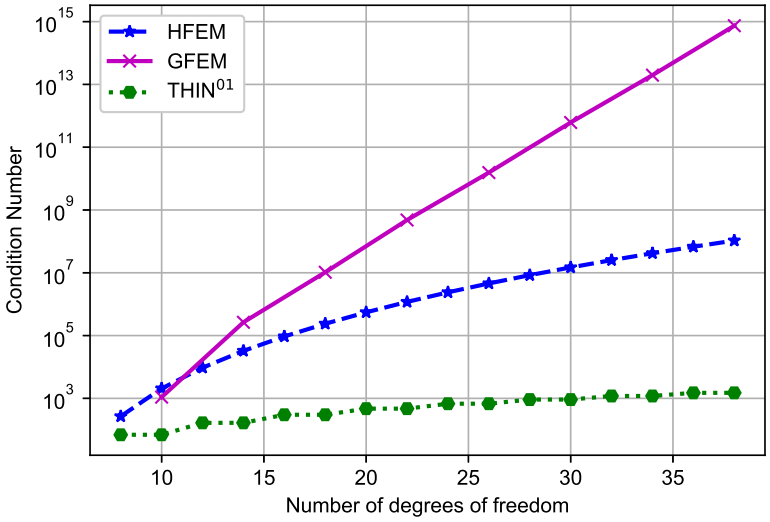

Figure 9 – Mass matrix's condition number.

The GFEM, although presenting the best convergence rate, shows a very accentuated increase in the mass matrix's condition number which may indicate an ill conditioning of the problem, which can cause negative eigenvalues to arise. The *p* Fourier, although presenting the lowest convergence rate, has the lowest growth of the condition number indicating a better conditioning of the problem.

As the modes of vibration are rarely found in the literature they are shown in Fig. 10, 11, 12 and 13. The plotted modes were obtained with the GFEM, but they are very similar to the modes obtained by the other methods.

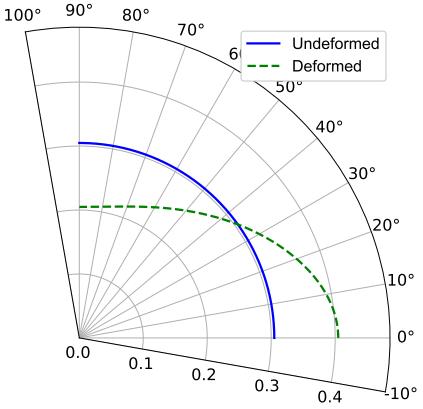

Figure 10 – Second vibration mode of the ring.

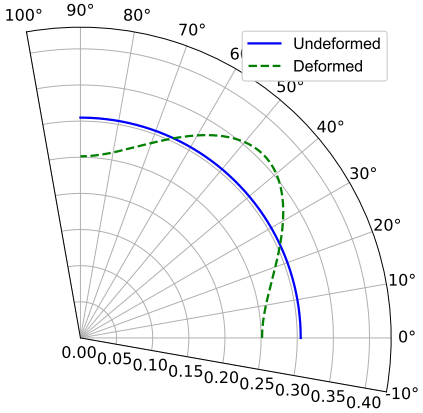

Figure 11 – Fourth vibration mode of the ring.

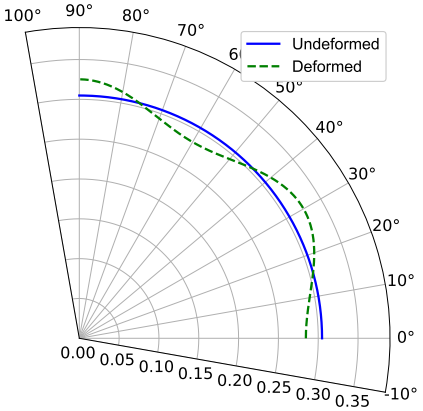

Figure 12 – Sixth vibration mode the ring.

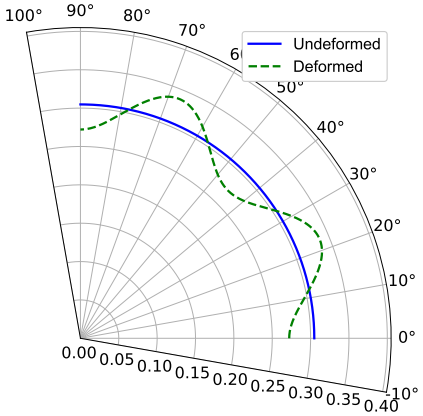

Figure 13 – Eighth vibration mode the ring.

Pinned-pinned arch model

A second model was implemented in order to evaluate efficiency of the methods. A pinned-pinned arch is analyzed as shown in Fig. 14. No analytical solution was found in the literature for pinned-pinned archs.

The modeled arch has the following properties: area of 4 m^2, moment of inertia of 0.01 m^4, radius of curvature of 0.75 m, material density of 2777 kg/m^3 and Young's modulus of 70×10^9 N/m^2. The results of the first ten frequencies are shown in Tab. 1 , and all models have 38 degrees of freedom.

The results indicate that the numerical values for the frequencies obtained with the GFEM are better, although very close to those obtained with HFEM. The $THIN^{01}$ method presents results slightly worse than the other two methods.

The first four modes are shown in Fig. 15, 16, 17 and 18.

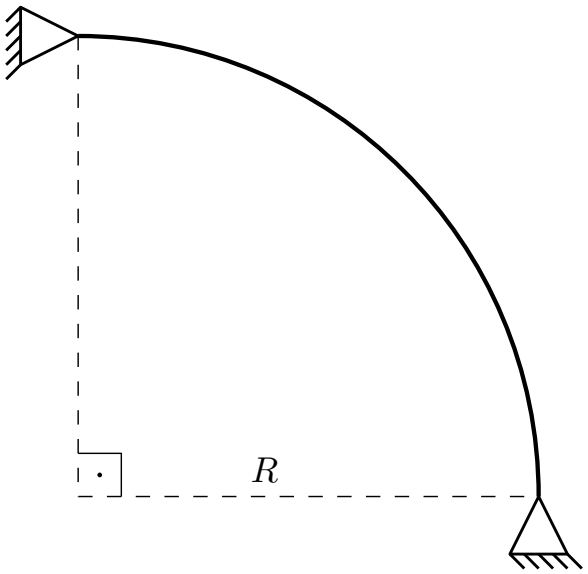

Figure 14 – Pinned-pinned Arch scheme.

Table 1 – Frequency (Hz) obtained by 3 hierarchical methods.

Mode	GFEM	HFEM	THIN^{01}
1	945.535087	945.535087	945.740900
2	975.817132	975.817132	975.848175
3	2368.383982	2368.383982	2368.402672
4	2426.636981	2426.636981	2427.246211
5	4391.158430	4391.158430	4392.770454
6	4420.755875	4420.755875	4420.771392
7	6553.845690	6553.845690	6553.846942
8	6874.683104	6874.683104	6879.171206
9	8740.930597	8740.930598	8741.009805
10	9765.570912	9765.570994	9772.482097

CONCLUSIONS

The convergence test performed on the one quarter ring model shows that the GFEM has the best convergence rate, remaining with a minor error in practically all analyses of the Fig. 5, 6, 7 and 8. The HFEM appears with the second highest convergence rate in general, but it can be noted that its convergence rate decreases for higher modes as shown mainly in the Fig. 7 and 8.

The *p*-Fourier element (THIN^{01}) presents the worst convergence rate, but when the evolution of the mass matrix's condition number is observed, it presents the best results, with the condition number not presenting accentuated growth with the refinement. The GFEM presents the most accentuated growth in the condition number.

The pinned-pinned arch model result highlights that the GFEM and HFEM have a higher convergence rate, because as it is known, the approximate results for the frequencies are always greater or equal to the analytical solution, so if the results are smaller they must be closer to the analytical solution.

Tab. 1 indicates that the ninth and tenth frequencies have slightly better results in the GFEM, which also reinforces that the HFEM has worse results at higher frequencies.

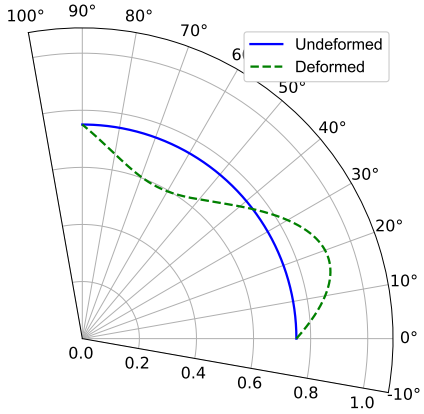

Figure 15 – First vibration mode of the arch.

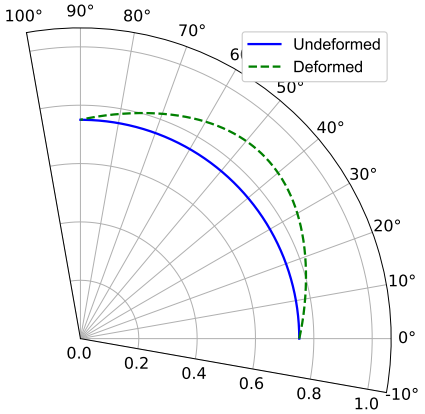

Figure 16 – Second vibration mode of the arch.

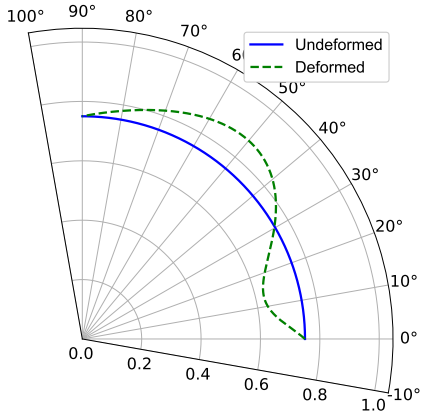

Figure 17 – Third vibration mode of the arch.

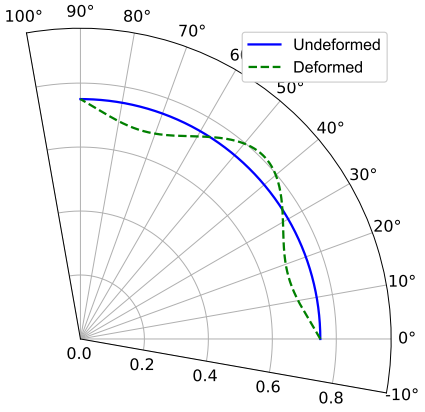

Figure 18 – Fourth vibration mode of the arch.

REFERENCES

Arndt, M., Machado, R. D. and Scremin, A., 2010, "An adaptive generalized finite element method applied to free vibration analysis of straight bars and trusses", Journal of Sound and Vibration, Vol. 329, No. 6, pp. 659–672.

Babuska, I., Banerjee, U. and Osborn, J. E., 2004, "Generalized finite element methods: main ideas, results, and perspective", International Journal of Computational Methods, Vol. 1, No. 67, pp. 67–103.

Campion, S. D. and Jarvis, J. L., 1996, "An investigation of the implementation of the p-version finite element method", Finite Elements in Analysis and Design, Vol. 23, pp. 1–21.

Dawe, D. J., 1974, "Numerical studies using circular arch finite elements", Computers and Structures, Vol. 4, pp. 729–740.

Duarte, C. A. M., Babuska, I. and Oden, J. T., 2000, "Generalized finite element methods for three-dimensional structural mechanics problems", Computers and Structures, Vol. 77, pp. 215–232.

Duarte, C. A. M. and Oden, J. T., 1996, "An h-p adaptive method using clouds", Computer Methods in Applied Mechanics and Engineering, Vol. 139, pp. 237–262.

Leung, A. Y. T. and Chan, J. K. W., 1998, "Fourier p-Element for the analysis of beam and plates", Journal of Sound and Vibration, Vol. 212, No. 1, pp. 179–185.

Leung, A. Y. T. and Zhu, B., 2004, "Fourier p-elements for curved beam vibrations", Thin-Walled Structures, Vol. 42, pp. 39–57.

Melenk, J. M. and Babuska, I., 1996, "The partition of unity finite element method: Basic theory and applications", Computer Methods in Applied Mechanics and Engineering, Vol. 139, pp. 289–314.

Oden, J. T., Duarte, C. A. M. and Zienkiewicz, O. C., 1998, "A new cloud-based hp finite element method", Computer Methods in Applied Mechanics and Engineering, Vol. 153, pp. 117–126.

Petyt, M. and Fleischer, C. C., 1971, "Free vibration of a curved beam", Journal of Sound and Vibration, Vol. 18, No. 1, pp. 1–30.

Raveendranath, R., Singh, G. and Pradhan, B., 2000, "Free vibration of arches using a curved beam element based on a coupled polynomial displacement", Computers and Structures, Vol. 78, pp. 583–590.

Timoshenko, S., 1955, Vibration Problems in engineering, 4th ed., Van Nostrand, New York.

Torii, A. J. and Machado, R. D., 2012, "Structural dynamic analysis for time response of bars and trusses using the generalized finite element method", Latin American Journal of Solids and Structures, Vol. 9, No. 3, pp. 1–31.

Weinhardt, P. O., Arndt, M. and Machado, R. D., 2016, "GFEM stabilization techniques applied to transient dynamic analysis", Proceedings of the XXXVII Iberian Latin American Congress on Computational Methods in Engineering, Brasília, DF, Brazil.

RESPONSIBILITY NOTICE

The authors are the only responsible for the printed material included in this paper.